

Using satellite imagery to map rural marketplaces and monitor their activity at high frequency

Tillmann von Carnap^{1,4*}, Reza M. Asiyabi^{2,3}, Paul Dingus⁴, Anna Tompsett^{5,6}

Affiliations:

¹ Department of Economics, University of Oslo; Oslo, 0851, Norway

² Mistra Center for Sustainable Markets, Stockholm School of Economics; Stockholm; 11350; Sweden

³ School of GeoScience, University of Edinburgh; Edinburgh; United Kingdom; EH8 9XP; United Kingdom

⁴ Center on Food Security and the Environment, Stanford University; Stanford, 94305, United States of America.

⁵ Beijer Institute of Ecological Economics, The Royal Swedish Academy of Sciences; Stockholm; 10405; Sweden

⁶ Institute for International Economic Studies, Stockholm University; Stockholm; 10691; Sweden

*Corresponding author. tillmanv@econ.uio.no

Author contributions:

Conceptualization: TC

Methodology: TC, RA, PD, AT

Investigation: TC, PD, AT

Funding acquisition: TC, AT

Writing – original draft: TC

Writing – review & editing: TC, RA, PD, AT

Competing interests: Authors declare that they have no competing interests.

Classification: Social Sciences - Sustainability Science

Keywords: rural marketplaces; remote sensing; economic activity; monitoring

This PDF file includes:

Abstract

Main Text and Figures

Funding acknowledgement

References

Supplementary Materials

Abstract: In many rural areas of low- and middle-income countries, weekly gatherings of buyers and sellers are the most tangible manifestation of the market economy. Knowing these markets' whereabouts and activity over time could provide insights in otherwise data-scarce environments, helping researchers and policymakers to better understand poor rural economies. But these markets are by nature informal and scattered widely across often-remote regions. As a result, data on this fundamental institution is sparse and inconsistent. We develop, test, and apply a method to fill this gap, leveraging market activity's unique temporal and visual signature in satellite imagery. Using secondary data from Kenya, Malawi, and Mozambique, we first confirm that we detect markets with high sensitivity and specificity. We then derive a map of 1,712 markets in Ethiopia and track their activity at up-to-weekly frequency between 2017 and 2024. Measured market activity exhibits seasonal patterns following local agricultural calendars and responds to weather and conflict shocks. Our approach requires no ground-truth data, is applicable wherever periodic markets exist, and can be fully automated to produce an up-to-weekly measure of economic conditions in areas where such data is otherwise generally not available.

Introduction

Across much of the world, buyers and sellers of goods and services gather to trade in specific locations on specific days. Such periodic markets simplify the identification of trading partners where populations live dispersed, allow for the bulking of goods where individual transport is uneconomical, and enable face-to-face transactions where weak legal systems complicate contracting¹. The conditions making periodic markets an efficient mode of exchange applied from the dawn of trading systems until the industrial era, and they still do in rural areas of many developing economies today²⁻⁴. Consequently, periodic markets have been documented across pre-historic societies from the Roman Empire to pre-colonial West Africa to Mughal-era India⁵⁻⁷, and they remain widespread today.

The same conditions that make it efficient to trade at periodic marketplaces also make associated data extremely scarce. Because they are rural and informal, consistent maps are typically not available, nor is market attendance recorded over time. This prevents researchers from gaining a deeper understanding of how these markets evolve and respond to external factors that potentially trigger economic growth. Beyond a better understanding of markets *per se*, changes in activity could also be informative about changes in economic conditions more broadly. Where a large share of local trade occurs at such marketplaces, busier market days reflect more income spent, more goods traded, or both.

In this paper, we develop, test and apply a method that addresses these gaps by using high-frequency satellite imagery to map periodic marketplaces and track their attendance over time. Our approach relies exclusively on satellite imagery and applying it does not require any prior information about market locations. Instead, we rely on markets' highly distinctive visual and temporal signature in stacks of images.

To evaluate how successfully we detect markets, we would ideally use up-to-date, internationally comprehensive market maps. Similarly, we would ideally evaluate our activity measure using

high-frequency local measures of economic activity. Such data largely do not exist, however, and their absence motivates our work. We make progress by validating our market detection method with secondary data from Kenya, Malawi, and Mozambique. We then apply the method to derive a novel map of 1,712 marketplaces in Ethiopia, and an activity panel for these markets between 2017 and 2024. No method could detect every market, given that the term can informally describe anything from a handful of individual stalls selling small quantities of goods to large, urban wholesale operations. We detect a particular but widespread type of market: occurring periodically, during daylight hours, and at least partially in the open air. We then show that our measure of market activity correlates within and across seasons with local rainfall, a known determinant of rural economic activity⁸. Lastly, we illustrate the method's usefulness for locally specific monitoring independent from ground conditions with an application to recent violent conflict in Ethiopia.

Our approach has several potential applications. Better information about markets' locations can help policymakers design more effective rural development policies, such as improvements to rural transport systems. High-frequency information about market activity can also help generate timely feedback about the success or otherwise of different interventions designed to promote market integration, a stated goal of many development policies. High on-the-ground data collection costs otherwise make it difficult to evaluate which programs work or how to improve program design. Finally, our data can be integrated into early-warning systems in contexts where on-the-ground information on economic conditions is too costly, or unsafe, to obtain.

More broadly, tracking rural marketplaces with satellite imagery presents unique advantages for monitoring in remote economies and significantly expands the toolkit available to practitioners⁹. Other sources of information, such as enterprise or household surveys, are infrequently collected, spatially sparse, and costly to scale. In contrast, modern satellite imagery combines high spatial resolution with dense geographical and temporal coverage^{10–12}. Absent cloud cover, satellites capture near-daily images of every outdoor marketplace worldwide. Satellites also collect data

continuously and consistently regardless of local conditions, ensuring comparability across space and time. Finally, and unlike survey data, satellite images are available in real-time, and processing can be fully automated. This provides an unprecedented ability to monitor rapidly evolving situations, including in conflict-affected settings like the Ethiopian example we study.

Existing applications of satellite data to learn about economic conditions in low-income countries implicitly or explicitly infer conditions from large assets that are visible from space, such as buildings or infrastructure^{13,14}. These assets evolve slowly, however, and the derived indicators can hence be slow to pick up even substantial changes in economic conditions. Furthermore, light emissions at night – a commonly used proxy for economic development – can neither discern variation in living standards among the poorest^{13,15}, nor does it reliably pick up short-term changes¹⁶. Consequently, existing approaches based on satellite imagery have to date primarily informed comparisons across space or over long periods. In contrast, marketplace activity can visibly change every week, providing the spatial and temporal granularity needed to measure short-term responses to economic shocks or policies, or potentially inform the rapid targeting of assistance¹⁷.

In summary, this paper demonstrates how to detect marketplaces and track their activity using globally available near-daily satellite imagery. Using widely accessible data, our method can produce temporally and geographically fine-grained measures of a central feature of rural economic activity.

Detecting and tracking marketplaces

Detecting and tracking marketplaces requires substantial amounts of imagery as well as processing capacity. When identifying marketplaces, we therefore focus our search on ‘candidate locations’, i.e., areas that have a relatively high *ex-ante* likelihood of containing marketplaces, such as villages or roadsides, as opposed to unpopulated areas. Given a candidate location, we detect marketplaces as follows.

The basic intuition for our approach is that marketplaces appear differently on market days and non-market days, as shown in very-high-resolution (VHR; 30cm) images for a candidate location in Mozambique (Fig. 1A). At this resolution, colourful market structures and attending crowds are clearly visible on a Sunday, the local market day, and conspicuously absent on a Wednesday.

Acquiring such VHR imagery at scale is prohibitively expensive, however, and available images only sporadically capture market days. Instead, we use lower resolution (3.1m) PlanetScope RGB imagery that is globally available with a median average revisit interval of 30 hours¹⁸. In an individual Sunday image at this lower resolution (Fig. 1B), market activity at the same location is barely visible as a patch of relative darkness. We can nonetheless detect a temporal signature because, in an imagery stack, appearance differences that are associated with market activity occur *regularly*, on market days. In contrast, other appearance differences, such as those arising from the ploughing of fields or wetting of soils, occur more unpredictably.

To isolate the periodic appearance differences that characterise market activity from other changes, we would ideally use imagery from the same location on a non-market day as a reference. As we do not know market days beforehand, we instead build on the intuition that, for markets that occur fewer than half the days in a week, a median composite of sufficiently many images will resemble a non-market day. We therefore construct for each image a reference composite using imagery from surrounding dates. Subtracting this composite yields a difference image with areas highlighted that appear unusual for the given period, reducing in particular the influence of seasonal vegetation changes (Fig. 1C). Averaging these difference images by day-of-week yields a representation where pixels with periodic changes on a given day-of-week exhibit higher values than those whose appearance does not vary at this frequency (Fig. 1D).

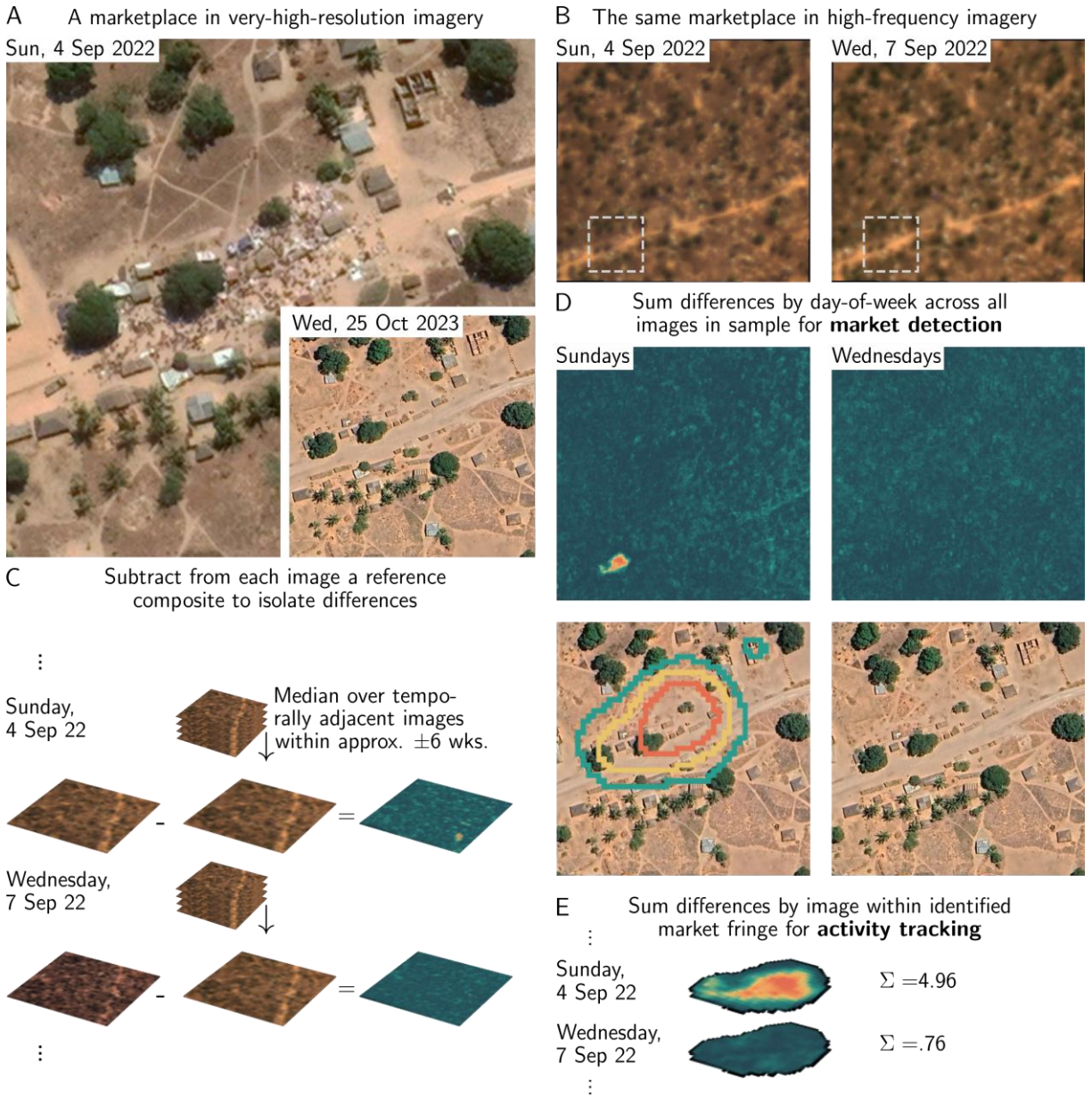


Fig. 1: Method intuition & sequence. (A) A marketplace in Nangata, Mozambique (14.21°S, 40.7°E) as seen in the Google Earth Archive on a non-market day (Wednesday) and a market day (Sunday). Market activity is discernible as crowds, stalls, and vehicles in the Sunday image. (B) The same location on a Sunday and a Wednesday in PlanetScope imagery. (C-E) Illustration of workflow for market detection and activity tracking. Individual PlanetScope images between June 2016 and September 2023 are differenced with median composites from temporally adjacent images – approximating the appearance on a non-market day – to isolate appearance differences due to market activity (C). Aggregate differences per day-of-week identify market

shapes at various threshold levels (D). The high-resolution images show the area in which market shapes are detected at various threshold levels. Market activity readings within these shapes are derived by summing differences across pixels within each shape and image (E). We then select as the market area the largest shape in which the median reading across market days exceeds the 75th percentile across non-market days.

Across marketplaces, market-day activity varies in its appearance compared to non-market days. Sometimes it is brighter than the otherwise bare ground, sometimes darker; vendors often use temporary structures of distinctive but locally idiosyncratic colours. We address this heterogeneity by aggregating the information in each pixel of each day-of-week difference image into a summary measure of brightness and colour differences. Specifically, we multiply the maximum absolute difference of values across the red, green, and blue bands – tracking brightness variation – with the maximum absolute difference of angles in a polar representation of the image¹⁹ – tracking colour variation.

We identify contiguous areas where the signal from combined brightness and colour differences exceeds predefined thresholds and tune these thresholds using ground truth data (see following section). While this procedure could potentially identify other periodic events like religious gatherings, we confirm below that we indeed predominantly detect marketplaces.

Given the available imagery and our choices in designing the algorithm, our approach will identify markets that meet the following criteria: i) occurring periodically (e.g., one, two or three market days per week); ii) at least partly taking place in the open with a detectable footprint of at least 50m²; iii) operating sufficiently frequently between June 2017 – when imagery becomes consistently available – and September 2024 – our cutoff date – to distinguish activity from background noise; (iv) and operating around 10:30 AM local time when most imagery is captured. We discuss the implications of these criteria for our method’s coverage and generalizability when we introduce the novel Ethiopian market map.

We now turn to measuring activity over time. Marketplaces typically feature a core with relatively stable activity and a fringe with seasonal or other fluctuations, but their relative positions vary across markets. We first identify each marketplace's fringe by creating a series of concentric rings originating from the part of the market with the strongest periodic signal. Within each ring and for each image, we compute the mean of brightness and colour differences as above. We then define the fringe of each marketplace as the largest ring where the median measure across market days exceeds the 75th percentile of non-market days. Intuitively, this should identify areas where activity does fluctuate – as opposed to more constant activity in the market's core – while at the same time limiting the influence of noise from adjacent areas that markets rarely or never expand into. For each available image, our preferred measure of activity is then the mean of the brightness and colour differences across pixels within the area constituting the outer boundary of the fringe (Fig. 1E). This measure reflects the density of structures, vehicles and crowds on market days within the typical market area. The resolution of the underlying imagery does not allow us to discern the components separately.

The derived metrics of appearance differences originate from heterogeneous marketplace layouts, and their absolute values are therefore not directly comparable across marketplaces. To create an index that can be compared across marketplaces, we normalize these metrics by market and day-of-operation with their average during a specific reference year. We adjust for varying relative frequency of images throughout the year (see Fig. 3B) so that the index corresponds to an annual average of market activity.

Limited validation data suggests successful detection of markets

We now assess the accuracy of our detection method. Using the limited available sources of validation data, we confirm that we successfully detect known marketplaces and that detected areas overwhelmingly correspond to trading locations rather than other periodic events.

To validate our detection procedure, we use secondary datasets from Kenya²⁰, Malawi²¹, and Mozambique²². These datasets are uniquely useful in that they originate from exercises specifically targeting periodic marketplaces, listing the coordinates and days of operation for 60, 31, and 48 marketplaces, respectively, with 1.2 market days per market on average (Fig. S1). For each listed location, we outline candidate locations by manually drawing polygons around the settlement surrounding the marketplace coordinates, at an average size of 181ha.

The validation datasets let us directly test our ability to detect periodic markets where they are known to exist. However, we lack maps of otherwise comparable locations without marketplaces. To examine how frequently we erroneously detect markets, we use imagery from designated non-market days as pseudo-instances of such locations. Specifically, we remove all images of designated market days for a given location from its imagery sample, replacing them with randomly sampled images from designated non-market days. The resulting set of imagery should approximate the appearance of an otherwise comparable location without a periodic market. We then calculate the share of these pseudo-locations that are erroneously identified to have a market on any day ('false positive rate' (FPR)). Within the original set of locations, we calculate the share of location-day tuples that are correctly detected ('recall') and the share of detected tuples that are designated market days for a given location ('precision').

Despite varying economic and agro-ecological settings and across a broad range of the tuning parameter, we achieve precision above 90% in the sample of locations with marketplaces, and an FPR below 10% in the sample of pseudo-locations without marketplaces (Fig. 2). The detected shapes are small in relation to the initial candidate locations (mean market area share of candidate location area 3.5% (median: 1.6%). This suggests that even when screening relatively large locations, appearance differences on market days will, if present, stand out clearly against other potentially present periodic appearance changes. Taken together, high precision and low FPR underline our ability to derive geographically comprehensive and consistent maps of marketplaces that enable subsequent activity monitoring.

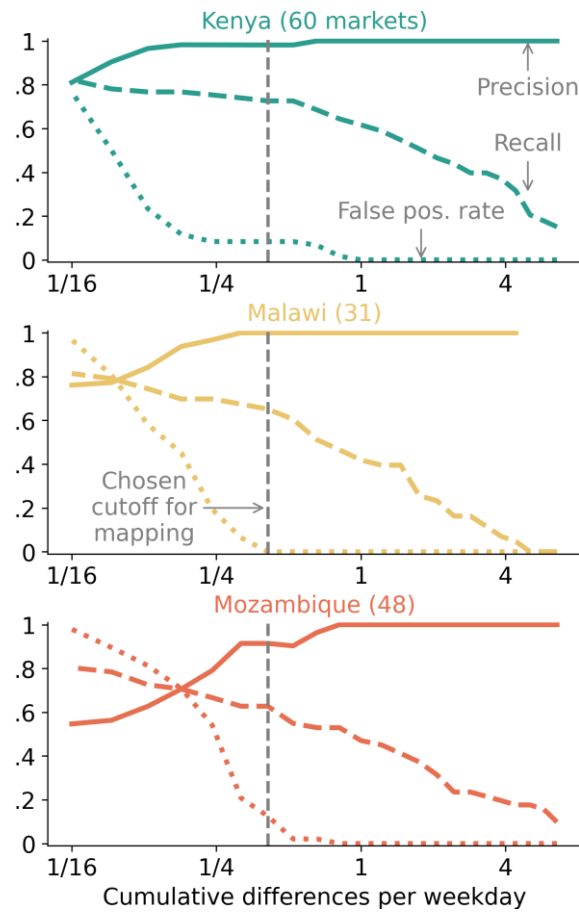


Fig. 2: Validation of market detection against ground-based marketplace maps. Precision, recall and false positive rate (the share of pseudo non-market locations for which the algorithm erroneously detects any marketplace) across market datasets from three countries. The horizontal axis indicates a range of possible threshold values at which aggregate periodic deviations would be considered a market shape. The vertical line at 0.41 identifies the chosen threshold for the mapping exercise underlying the subsequent activity analyses.

Recall rates decrease with stricter thresholds and never reach 100%, driven by locations where we do not detect activity on designated market days. Several factors may contribute: first, although we intentionally select datasets that list marketplaces with distinct designated market days, some marketplaces may also have similar levels of activity on other days of the week, complicating their detection. Second, some coordinates, particularly in Mozambique, refer to large trees, which often serve as local gathering places. Periodic activity may indeed happen in their

shade, which would not be detectable in remotely sensed imagery. However, it is likely on a substantially smaller scale than the markets we successfully detect. Finally, the datasets were collected at different times. Only markets that were active for a sufficiently large share of our imagery period will be detectable. These factors do not reflect shortcomings of our specific validation data but intrinsic challenges when studying such a dynamic and diverse phenomenon. No current approach can detect and monitor economic hubs of *all* forms and sizes. Our approach allows detection and monitoring of a consistently defined group.

Regarding potentially misidentified marketplaces, our method demonstrates high precision and a low false positive rate at higher threshold values. We can investigate the types of phenomena inducing false positives at lower threshold values by overlaying detected shapes onto VHR imagery. At the threshold indicated in Fig. 2, we identify two cases in Kenya where livestock pens adjacent to marketplaces are detected on days immediately before or after designated market days – likely livestock brought to the market in advance or awaiting transport after sale – as well as one possible instance of a repeated gathering in front of a public building.

A map of periodic markets in Ethiopia

We focus the remainder of the paper on a novel panel of marketplace activity in Ethiopia. This dataset allows us to characterise the regions where markets' activity is informative about economic conditions and to examine the sensitivity of their measured activity, as well as to illustrate an application of our approach to tracking disruptions caused by recent conflict.

To define candidate locations for the map underlying the activity panel, we replicate the approach shown in Fig. 1B-D with Sentinel-2 imagery, which comes at a lower resolution and frequency, but is much cheaper to access and process. We limit our search to areas within 300m of roads recorded in OpenStreetMap, or where the Global Human Settlement Layer²³ suggests built-up area. These restrictions focus our attention to areas where markets can reasonably be expected, rather than scanning vast areas of agricultural or natural vegetation. We also exclude Addis

Ababa, since markets in very large cities are less likely to be periodic as higher aggregate economic activity can sustain permanent, more formal trading systems¹, and there are more confounders for our approach, such as periodically-filling parking lots. We draw polygons with a buffer of 250m (mean size: 24ha) around areas of elevated periodic appearance differences in the Sentinel-2 imagery and rank the resulting candidate locations (Fig. S2) by the strength of the difference. We then screen locations in decreasing order of the difference signal using the higher-resolution and higher-frequency PlanetScope imagery.

To have the market map be as accurate as possible, we make use of the fact that marketplaces typically have intuitive layouts and locations, such as along roads or on village squares. We assess the shapes returned by the screening procedure by superimposing them onto VHR imagery to include false negatives – where the appearance differences do not pass the chosen threshold – and exclude false positives – elevated appearance differences in locations that are apparently not marketplaces. The latter include periodically-filling parking lots or storage areas around industrial operations, as well as artefacts resulting from noise. We continue the screening and quality control process until screening becomes uneconomical, i.e. the share of candidate locations returning a marketplace falls below 10% (Fig. S3A). To illustrate the gains in accuracy by our manual examination for false positives and false negatives, 97.3% of detections with signal strength above the threshold from Fig. 2 are ultimately classified as marketplaces, while 19.5% of all eventually confirmed marketplaces were initial ‘false negatives’ that we reclassify (Fig. S3B).

Following this procedure, we detect 1,712 markets with 1.08 days of operation and covering .87ha, on average (Fig. 3A; see Fig. S4 for example detections). The detected markets are spread widely across the populated parts of the country outside the major cities – 72.5% of the population outside Addis Ababa live within 10km of a marketplace (Fig. 3B). With markets distributed throughout most of the country, the market activity measures will be most useful for economic monitoring in rural areas – home to 77% of the population²⁴ – where existing data is most scarce. There are also large parts of the country where we do not detect many periodic markets,

especially in the eastern Afar and Somali regions. This likely reflects the regions' lower population densities, as well as their economies' pastoralist and semi-nomadic character.

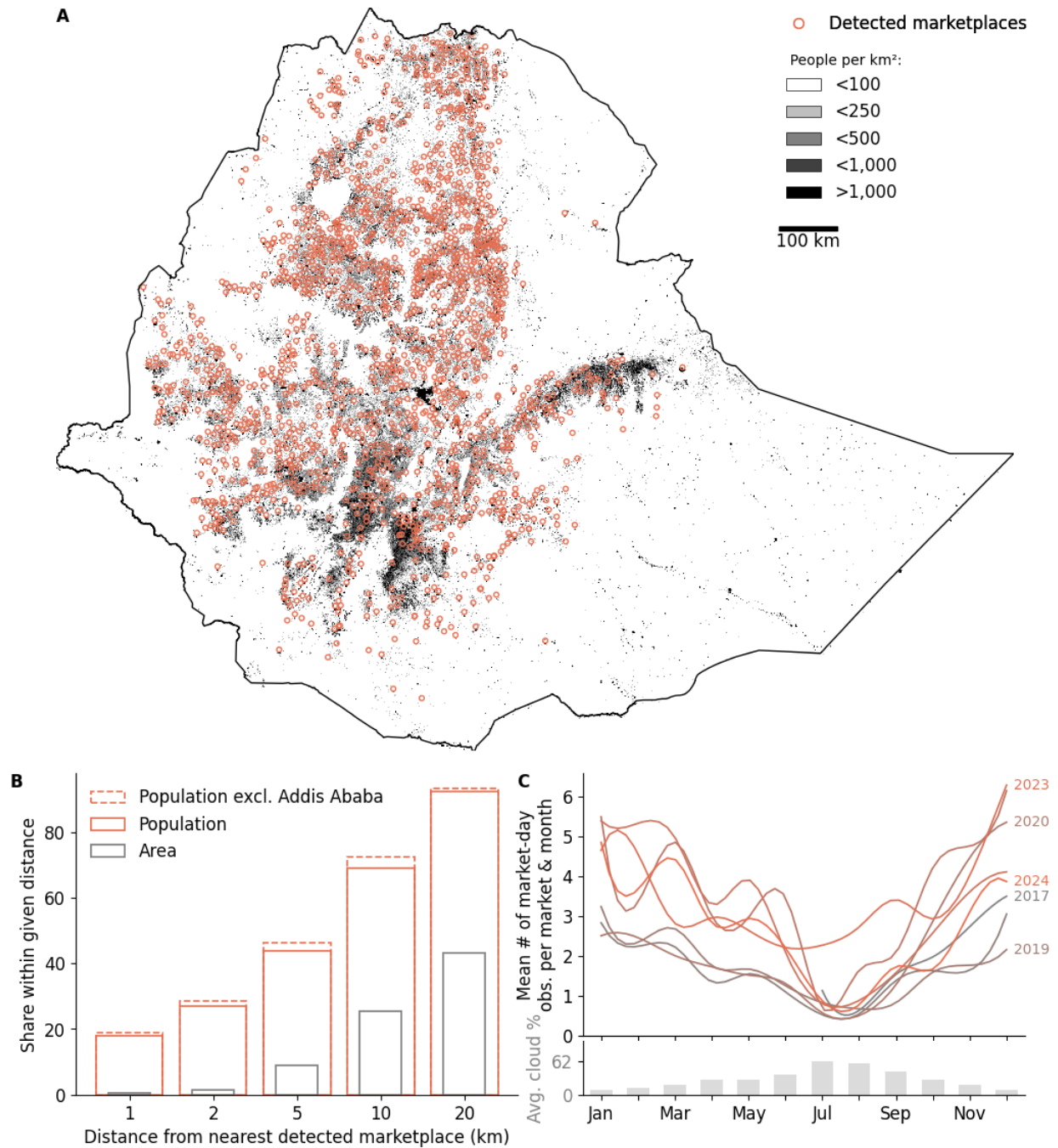


Fig 3. Spatial and temporal coverage of a novel marketplace map of Ethiopia. (A) The map shows the marketplaces detected through a country-wide screening using our method, superimposed on high-resolution population density data³. Addis Ababa was excluded from the

screening. (B) Shares of population (including and excluding Addis Ababa) and country area lying within various distances from detected marketplaces. (C) The figure shows smoothed averages of the count of market-day activity measures across the Ethiopian sample for each year in our panel. Availability is driven by satellite launch dates, seasonal cloud cover, and the number of active market days. The bottom panel shows the average share of pixels classified as cloudy in Sentinel-2 imagery between 2018-2024 across our detected marketplaces.

The technical parameters of our approach define the subset of markets we detect among all locations that may colloquially be referred to as ‘markets’. To be observable, trading must occur periodically, open-air and around 10:30am local time when the bulk of imagery is acquired. Fig. 3A shows that these criteria apply to markets over a wide geographical range. This prevalence of detectable markets is not merely a fortunate coincidence, however, but rather an adaptation of the trading system to local contexts: midday gatherings accommodate participants traveling from surrounding areas, whereas markets held in the early morning or evening tend to serve nearby residents, as is often the case in denser urban environments. Likewise, convening on fixed, publicly known days increases the likelihood of finding trading partners in otherwise thin markets and allows time between market days for goods production. These advantages are evident in the operational patterns of detected markets: 92% operate once a week, 7% twice a week, and only 0.4% three times. Finally, while open-air markets are the norm, many of the detected areas encircle what are likely fixed market structures, illustrating that even when markets are partly covered, activity spills into surrounding areas where it is detectable (Fig. S4).

A possible confounder we did not yet discuss could be religious gatherings that also follow a weekly cycle. However, only one of the 1,712 detected locations lies within 50 metres of a religious building registered in OpenStreetMap and has a signal we detect on days of worship (Tab. S1). This low rate of false positives from religious gatherings is likely because religious gatherings typically occur indoors and at substantially smaller scales than marketplaces.

Comparing our satellite-derived map to existing sources, we find that our approach detects many more marketplaces than currently registered in OpenStreetMap ($n = 428$) and a somewhat lower number than recorded in the last available census of marketplaces from 2007²⁵ ($n=2,627$). The inclusion criteria for the census are unknown, and many locations appear to be registered wrongly, with centroids that lie in dense vegetation or distant from population centres. In fact, we find a 3.4 times larger share of the population living within 1km of our, fewer, detected marketplaces, compared to the census ones (Fig. S5A). Furthermore, 35% of census marketplaces have less than 100 people living within 200m, more than ten times the share for the detected marketplaces (Fig. S5B). Taken together, these statistics suggest that the census locations are either not accurately registered, or record an entirely different phenomenon.

Equipped with this map of marketplaces, we can then derive the activity measure underlying the exercises in the remainder of the paper. The measure's availability over time primarily depends on the number of satellites in orbit, which increased after 2020, as well as seasonal cloud cover (Fig 3C).

Measured market activity varies with agricultural calendar and weather

Fig. 4A shows data for one marketplace over a three-week period. For this and the following exercises, we normalize the activity measure for each market by first subtracting the non-market day average in 2018, before dividing by the market-day average from the same year and multiplying with 100. This procedure ensures that 100 corresponds to the average detected activity on market days during the reference year of 2018, and 0 corresponds to the average detected activity on non-market days. As in the illustration of the approach in Fig. 1E, activity readings are markedly different on designated market days and non-market days. This level difference, as well as the clear separation of their ranges, would not appear if the raw activity readings did not clearly distinguish the extent of attendance on market days from their appearance

on non-market days. Fig. S6 confirms that measures differ significantly between market days and non-market days across most detected marketplaces.

Beyond registering market attendance, changes in market activity are potentially useful as a proxy for changes in local economic activity. When incomes are higher, more people will gather in the places where goods and services are available for purchase. Similarly, when more goods are being produced locally, more producers will also be drawn to those same locations, where buyers are to be found. While we lack market-level measures of attendance at sufficient temporal and spatial density for a direct validation, we expect our activity measure to respond to established locally relevant drivers of supply and demand. Given rural areas' reliance on rain-fed agriculture²⁴, we expect seasonal patterns of market activity to reflect seasonal patterns of rainfall⁸, peaking around and after harvest, when crops are sold. Fig. 4B illustrates this pattern for the 42 markets detected in the Central zone of the Tigray region. Activity is lowest early in the growing season – a period often referred to as the lean season²⁶ – and rises sharply towards the harvest season. Market activity's sharp and unseasonal decrease in April 2020 coincides with the imposition of restrictions in response to the Covid-19 pandemic²⁷.

One might be concerned that these seasonal patterns simply reflect environmental changes, such as varying vegetation or cloud cover. We verify that this is not the case by comparing variation in market day activity to variation in non-market day activity. The latter also varies over time, but with markedly different seasonal patterns, likely reflecting residual weather-related noise (e.g., clouds and their shadows appearing as brightness and colour differences). Importantly, non-market day seasonal fluctuations are substantially smaller in magnitude, suggesting that the observed seasonality in market-day measures reflects genuine changes in market activity (Fig. 4B).

The zone shown in Fig. 4B lies in a region with a strong unimodal rainfall cycle. Fig. 4C shows how the seasonal pattern of market activity differs across zones with different rainfall patterns, which in Ethiopia vary between unimodal and bimodal²⁸.

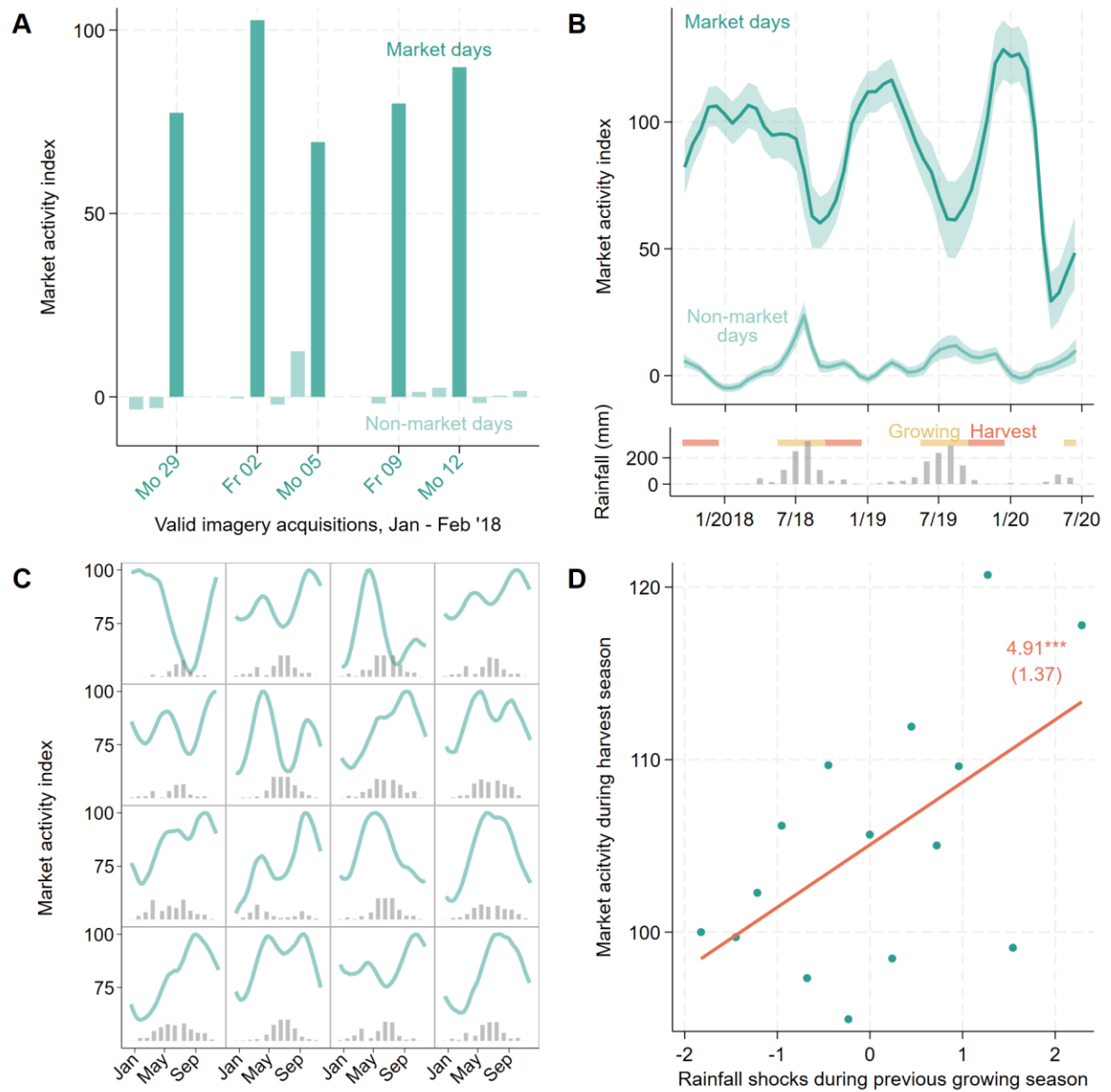


Fig. 4: Validation of activity tracking with Ethiopian sample markets. (A) Readings for market at 0.18°N, 34.3°E, where 100 (0) represents the average market activity in 2018 on market days (non-market days) from an interpolation of actual readings across the whole year to account for seasonal variation in image availability. (B) Smoothed averages and 95%-confidence intervals of

activity readings for 42 markets in Tigray's central zone, 7/2017-6/2020. The bottom panel shows average monthly rainfall across the marketplaces in the sample as measured in ²⁹. Growing and harvest season taken from ²⁸. **(C)** Smoothed 2018 averages for the 16 zones with the highest number of marketplaces. The top left panel corresponds to the zone shown in (B). Grey bars indicate monthly rainfall. **(D)** Binned scatter plot across zones, excluding Afar and Somali regions as pastoral areas with different production systems. Horizontal axis shows standardised rainfall shocks during June-August relative to 1998-2024 average; vertical axis shows average activity across markets (100 = 2018 average) for October-December in 2017-2024. Orange line represents linear fit from a regression with fixed effects for each zone. Standard errors clustered at the zone level.

The seasonality in market activity could, in principle, reflect people's taste for visiting the market at specific times, e.g., when it is not raining, rather than indicating changes in incomes. Beyond the inter-annual variation in Fig. 4B, however, we also see differences in activity levels across years, suggesting that market activity may also respond to other factors. One such driver could be variation in growing conditions for agricultural crops, which determine the abundance of harvests and, subsequently, the amount of crops households sell as well as their demand for consumer products sold at marketplaces. Harvest-season market activity should therefore increase in response to more abundant rainfall. Fig. 4D confirms this expectation for the 61 administrative zones during 2017-2024. The positive association we observe is likely an underestimate of the true relationship: we focus on the main growing and harvest seasons, but their precise onsets vary across space and time. Also, normal patterns of seasonality were disrupted in many zones during the study period due to conflict or the Covid-19 pandemic.

Taken together, these exercises highlight the ability of our remotely-sensed measure to detect meaningful changes in a proxy for economic conditions, including over short time periods such as during the 2020 lockdowns or when activity picks up around local harvests. As with most other metrics, whether we detect a signal depends on its strength relative to background noise. In our

data, noise arises from other sources of variation in images, such as haze, changing acquisition times or lateral distortions between images³⁰. Using the standard deviation of month-to-month differences across various sample definitions, we can estimate the sample size needed to statistically detect differences of a given magnitude (Fig. S7). Statistical power is higher with larger samples of markets or over longer time periods. For example, a year-on-year difference of 4 index points can be detected with 80% power in a sample of just four marketplaces, while detecting a month-on-month difference of the same magnitude requires a sample of around 40 marketplaces.

Market monitoring during a humanitarian crisis

Poverty is increasingly concentrated in fragile regions³¹. Fragility not only affects economic outcomes, but also our ability to monitor them, making it costly, or impossible, to collect field data or maintain consistent administrative records⁹. Our method has particular potential to remotely detect, quantify and anticipate disruptions in conflict-affected regions, when other sources of information are sparse.

We use our data to track the consequences of the recent episodes of conflict in Ethiopia during which period widespread instability hindered access to reliable information on economic conditions³². Starting in November 2020, civil war broke out in the Tigray region and the following years saw fighting and instability across large parts of Ethiopia. We combine detailed geo-referenced counts of conflict events³³ with our panel of market activity. Across the three regions with most recorded events, periods with elevated conflict generally coincide with lower market activity (Fig. 5A). We also observe sharp decreases in market activity around the imposition of Covid-19 restrictions in the second quarter of 2020, with decreases being most pronounced in the Tigray region.

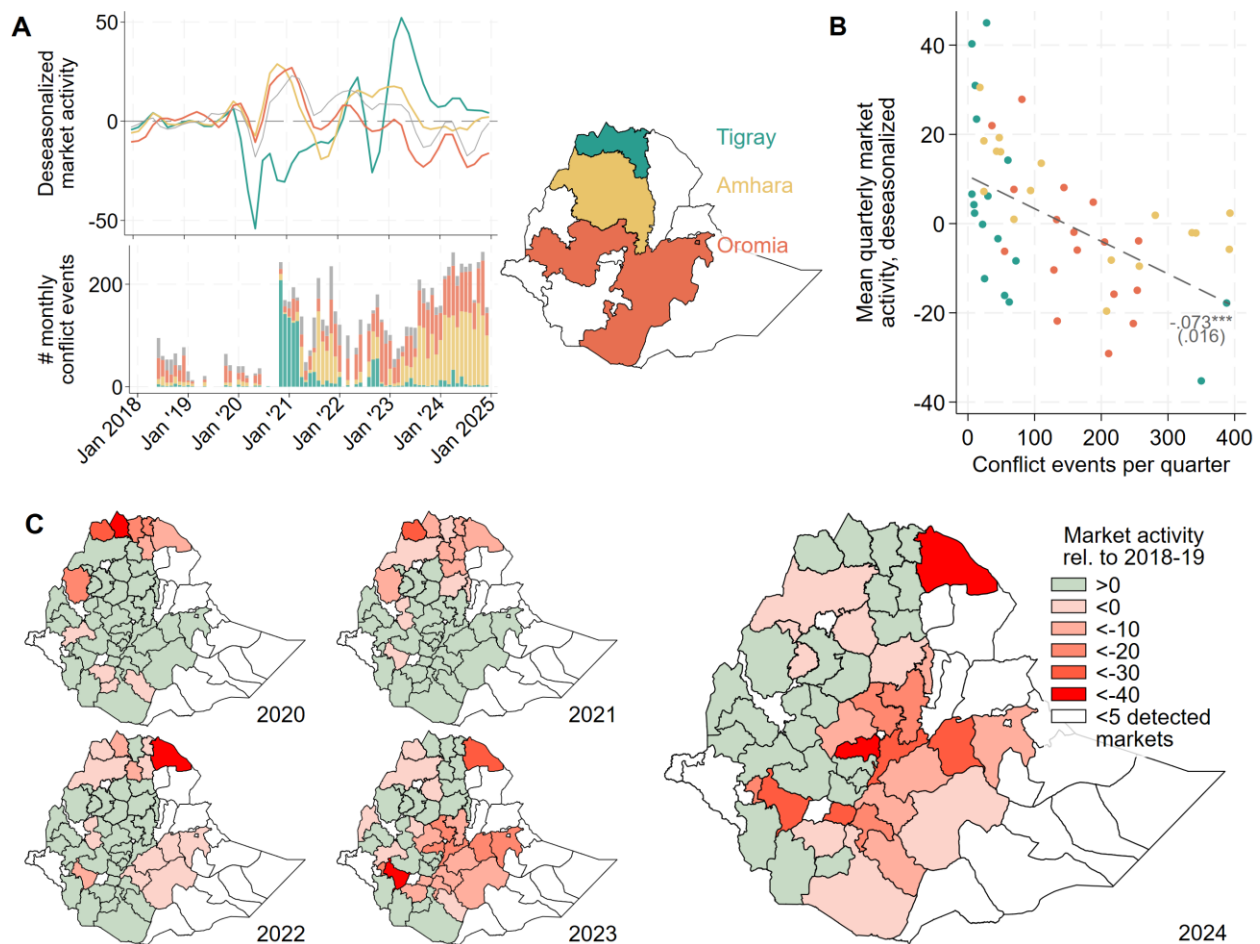


Fig. 5: Application of approach to country-wide monitoring in Ethiopia, 2018-24. (A) Market activity readings on market days across markets in three Ethiopian regions, deseasonalised according to their 2018-19 month-of-year averages, along with counts of conflict events by region. Grey lines and bars correspond to areas outside the three regions highlighted in the map. (B) Counts of conflict events and mean measures from (A) by region, quarter and year, starting from Q4 2020. The dashed line represents a linear fit, with the associated coefficient estimate from a regression with heteroskedasticity-robust standard errors. (C) Administrative zones shaded by average market activity measures from (A) per year. Regions with less than 5 detected markets are left empty. Administrative borders are taken from the FAO Global Administrative Unit Layers dataset, with some smaller neighbouring zones merged within the same region for easier interpretability.

We confirm this visual evidence of a negative association between conflict and market activity in a regression (Fig. 5B). The panel also highlights substantial variation in market activity for a given level of conflict. While some of this variation may reflect noise, it also suggests that remotely-sensed market activity measures can contain information on local impacts beyond the more readily available conflict records.

Beyond regional correlations, our data also allows for finer – including arbitrary – spatial disaggregation: such an exercise reveals substantial heterogeneity in market activity changes across administrative zones (Fig. 5C). The magnitudes here are substantial – a 30 index-point decrease as observed in many zones is similar in magnitude to the seasonal swings seen in Fig. 4C. This indicates that in some years and zones, market activity on average did not exceed levels typically observed during the lean season.

A future application of our approach could be to complement existing early-warning systems that aim to detect humanitarian crises in time to intervene or prepare a response. Existing early-warning systems lack direct measures of short-run changes in economic activity, and instead focus on predictors of drought or other extreme weather events, or rely on measures such as nightlights, which respond only sluggishly to changes in economic conditions. Remotely-sensed market activity can complement these measures by providing timely, location-specific information about economic activity, independent of ground conditions.

Discussion

Detecting and monitoring rural marketplaces with satellite imagery provides an unprecedented opportunity to study a fundamental economic institution. Tracking rural market activity also makes it feasible to monitor economic conditions in remote or conflict-affected regions in near-real time and at high frequency. Our approach has potentially broad applications: policymakers could use the data to better target short-run relief programs; humanitarian actors could incorporate the

measures in early-warning systems; and researchers could better understand the economic impacts of extreme events or policy changes in remote rural areas.

There are several limitations to our approach. First, limited ground-based panels of economic activity in general and market attendance specifically inhibit our ability to validate the activity measure against its direct on-the-ground counterpart. This prevents us from, for example, examining whether the elasticity between market activity and local economic conditions may be non-linear. Here, correlating our activity measure with other high-frequency measures such as mobile phone data appears promising. This elasticity might furthermore change over time as economies develop and formalize. While the activity measures can be constructed from 2017, further analyses could substitute space for time and carefully compare across places at different stages of economic development.

Second, elasticities could differ across marketplaces if, for example, our measure is more sensitive for markets that are entirely open-air, compared to partially-covered ones. Such heterogeneity would complicate comparisons across markets, or groups thereof, as a unit change in measured activity would correspond to differently sized changes on the ground for different groups. There are three potential strategies researchers could use to avoid drawing erroneous conclusions. First, making comparisons within units – such as individual marketplaces or groups thereof – such as in Fig. 4B will prevent bias from cross-market heterogeneity. Second, analyses can focus on signs of changes – e.g., calculating the share of markets in an area where activity is lower than during some reference period – which may be more reliable than focusing on magnitudes. Finally, comparisons across marketplaces are likely to be more informative when the marketplaces are similar. Researchers can use measurable features of the markets – such as their size and shape, their position relative to infrastructure, and their seasonality – to shed light on the degree of comparability of markets in different comparison groups.

Another limitation to the accuracy of measured market activity originates from the quality of the underlying imagery. While PlanetScope's resolution, frequency, and global coverage uniquely enable our approach, challenges remain: spatial misalignment between images, different spectral response functions between sensors, and imperfect cloud masking introduce idiosyncratic noise. Particularly in areas affected by cloud cover, this substantially affects market activity signals. Future sensors may allow for further improvements.

Finally, we designed our method to balance potential transferability across heterogeneous climatic and geographical contexts with the need to maintain reasonable computational loads. This may lead us to miss important local heterogeneities. For example, cattle markets appear characteristically dark in the satellite imagery, while most other markets appear relatively colourful, a difference we ignore by relying on absolute differences. Our approach could, however, be locally tailored to distinguish such kinds of markets – or areas within marketplaces – especially when only a small region or a specific period are of interest.

Generally, however, our method, in combination with the global availability of the required imagery, opens the door to a deeper understanding of a universal institution that is closely linked to people's livelihoods in remote rural regions.

Funding: We gratefully acknowledge support from Riksbankens Jubileumsfond Infrastructure for Research Grant IN22-0041, STEG Small Research Grant 64 and the IGC project grant MOZ-22258. This work was also supported by an FSE postdoctoral fellowship to TC.

References

1. Bromley, R. J., Symanski, R. & Good, C. M. The rationale of periodic markets. *Ann. Assoc. Am. Geogr.* **65**, 530–537 (1975).
2. Sheahan, M. & Barrett, C. B. Ten striking facts about agricultural input use in Sub-Saharan Africa. *Food Policy* **67**, 12–25 (2017).
3. Linard, C., Gilbert, M., Snow, R. W., Noor, A. M. & Tatem, A. J. Population distribution, settlement patterns and accessibility across Africa in 2010. *PLoS ONE* **7**, (2012).
4. Haggard, S., MacIntyre, A. & Tiede, L. The rule of law and economic development. *Annu. Rev. Polit. Sci.* **11**, 205–234 (2008).
5. Hill, P. Markets in Africa. *J. Mod. Afr. Stud.* **1**, 441–453 (1963).
6. de Ligt, L. *Fairs and Markets in the Roman Empire*. (Brill, Leiden, the Netherlands, 1993).
7. Gajrani, S. *History, Religion and Culture of India, Volume 5*. (Gyan Publishing House, 2004).
8. Miguel, E., Satyanath, S. & Sergenti, E. Economic shocks and civil conflict: An instrumental variables approach. *J. Polit. Econ.* **112**, 725–753 (2004).
9. Jaron Porciello *et al.* Comment: Averting hunger in sub-Saharan Africa requires data and synthesis. *Nature* **584**, (2020).
10. Donaldson, D. & Storeygard, A. The View from Above: Applications of Satellite Data in Economics. *J. Econ. Perspect.* **30**, 171–198 (2016).
11. Burke, M., Driscoll, A., Lobell, D. B. & Ermon, S. Using satellite imagery to understand and promote sustainable development. *Science* **371**, (2021).
12. Wuepper, D., Oluoch, W. A. & Hadi, H. Satellite Data in Agricultural and Environmental Economics: Theory and Practice. *Agric. Econ.* (2025) doi:10.1111/agec.70006.

13. Jean, N. *et al.* Combining satellite imagery and machine learning to predict poverty. *Science* **353**, 790–794 (2016).
14. Henderson, J. V., Storeygard, A. & Weil, D. N. Measuring economic growth from outer space. *Am. Econ. Rev.* **102**, 994–1028 (2012).
15. Gibson, J., Olivia, S., Boe-Gibson, G. & Li, C. Which night lights data should we use in economics, and where? *J. Dev. Econ.* **149**, (2021).
16. Asher, S., Lunt, T., Matsuura, R. & Novosad, P. Development Research at High Geographic Resolution: An Analysis of Night-Lights, Firms, and Poverty in India Using the SHRUG Open Data Platform. *World Bank Econ. Rev.* **35**, 845–871 (2021).
17. Sherman, L., Proctor, J., Druckenmiller, H., Tapia, H. & Hsiang, S. *Global High-Resolution Estimates of the United Nations Human Development Index Using Satellite Imagery and Machine-Learning*. (2023) doi:10.3386/w31044.
18. Roy, D. P., Huang, H., Houborg, R. & Martins, V. S. A global analysis of the temporal availability of PlanetScope high spatial resolution multi-spectral imagery. *Remote Sens. Environ.* **264**, (2021).
19. Ghosatlou, O. & Datcu, M. Hybrid GAN and spectral angular distance for cloud removal. in *International Geoscience and Remote Sensing Symposium (IGARSS)* 2695–2698 (2021). doi:10.1109/IGARSS47720.2021.9554891.
20. Bergquist, L. F. & Dinerstein, M. Competition and Entry in Agricultural Markets: Experimental Evidence from Kenya. *Am. Econ. Rev.* **110**, 3705–3747 (2020).
21. FEWS NET. *Malawi Enhanced Market Analysis Report*. (2018).
22. von Carnap, T., Christian, P., Tompsett, A. & Zwager, A. Route to Development: Impacts of Road Network Improvements on Agricultural Intensification in Mozambique. **RIDIE-STUDY-ID-5f0d3682b0446**, (2020).
23. Pesaresi, M. *et al.* Advances on the Global Human Settlement Layer by joint assessment of Earth Observation and population survey data. *Int. J. Digit. Earth* **17**, (2024).

24. World Bank. *Employment in Urban and Rural Ethiopia*. (2021).
25. Central Statistical Agency. *Ethiopia's Rural Facilities and Services*. (2011).
26. Hirvonen, K., Taffesse, A. S. & Worku Hassen, I. Seasonality and household diets in Ethiopia. *Public Health Nutr.* **19**, 1723–1730 (2016).
27. Harris, D. et al. *The Impact of COVID-19 in Ethiopia: Policy Brief*. (2021).
28. Famine Early Warning System Network. Seasonal Calendar. <https://fews.net/east-africa/ethiopia> (2025).
29. Copernicus Climate Change Service. ERA5-Land monthly averaged data from 1950 to present. Copernicus Climate Change Service (C3S) Climate Data Store (CDS) <https://doi.org/10.24381/CDS.68D2BB30> (2019).
30. Kington, J. & Collison, A. *Scene Level Normalization and Harmonization of Planet Dove Imagery*. (2024).
31. Corral, P., Irwin, A., Krishnan, N., Mahler, D. G. & Vishwanath, T. *Fragility and Conflict: On the Front Lines of the Fight against Poverty*. (Washington, DC: World Bank, 2020). doi:10.1596/978-1-4648-1540-9.
32. Weldegebriel, L., Negash, E., Nyssen, J. & Lobell, D. B. Eyes in the sky on Tigray, Ethiopia - Monitoring the impact of armed conflict on cultivated highlands using satellite imagery. *Sci. Remote Sens.* **9**, (2024).
33. Raleigh, C., Kishi, R. & Linke, A. Political instability patterns are obscured by conflict dataset scope conditions, sources, and coding choices. *Humanit. Soc. Sci. Commun.* **10**, (2023).
34. Planet Labs. *PlanetScope Product Specifications*. (2023).

Supplementary Materials

Materials and Methods

- Market detection
- Activity tracking
- Details of validation exercises and respective data collections
- Details of application

Figs. S1 to S8

Table S1

Data availability

Materials and Methods

Market detection

The following paragraphs provide more detail on how we get from a candidate location to, if a market is confirmed, a shape outlining market areas and a time series of activity measures. Overall, our design choices within this approach reflect the desire for transferability across geographical contexts, the limitations of sparse ground truth data, and the need to maintain reasonable computational loads for the approach to be applied at scale.

While the PlanetScope imagery would in principle allow for a true global screening for periodic appearance differences, such an approach would be prohibitively costly in terms of the necessary imagery and computation. For the purposes of the Ethiopian market map, we therefore began by identifying likely market locations from visual interpretation of very high-resolution imagery. These locations then allowed us to configure a country-wide screening mechanism building on mid-resolution Sentinel-2 imagery and using gridded population data and roads recorded in the OpenStreetMap to exclude unpopulated areas. For each of the manually identified locations, we drew polygons around areas that could conceivably host a market – including built-up and

adjacent areas but excluding waterbodies, forests and agricultural land. For the Sentinel-2 derived candidate locations, we buffered locations of elevated periodic appearance differences by 250 meters. Fig. S2 shows the resulting set of locations where we applied our algorithm.

Given a candidate location, we identify all PlanetScope Scenes that intersect the area of interest and, according to the provider, have less than 50 percent cloud cover across the whole image tile (287 to 637km², depending on the imagery generation). We restricted our search to RGB imagery acquired after June 1, 2016 and before September 30, 2024 and downloaded orthorectified surface reflectance analytical data (Level 3B products)³⁴. For a typical location this returns an initial sample of about 2,200 images. During the downloading stage, we make use of the provider's pipeline to spatially align images using a cloud-free, post-2020 image as an anchor. This addresses distortions of the imagery due to varying sensor angles during acquisition.

We then process the imagery in Google Earth Engine. We first aim to identify whether a given candidate location indeed has areas of periodic appearance changes. We begin by masking each downloaded image with the provider's 'usable data mask' ('UDM2') and filter the image collections to only include relatively clean images, covering at least 20 percent of the candidate location and being at least 80 percent shadow-, haze- and cloud-free across the whole image tile according to the imagery metadata (discarding about 10 percent of the initial sample). We furthermore exclude images that are acquired more than 30 minutes before or after the median acquisition time for each location to reduce the influence of differing lighting conditions (about 20 percent of the initial sample). We also filter out images with faulty colour representations, defined as images where the mean across pixel values within any of the red, green and blue bands is more than two standard deviations away from the mean of that statistic across all images (about 5 percent of the initial sample).

A complication stems from the two generations of satellites deployed by the provider during our sample period. Each generation operates with its own spectral response function, leading to the same colour on the ground being represented as different RGB values in images from either

generation. If not properly addressed, these colour differences may be mistaken by our approach as changes in market activity. During the downloading stage, we follow the provider's recommendation and spectrally align each image with Sentinel-2 imagery, harmonising colour representations in our imagery both across the two generations, and within each generation across individual satellites³⁰. Even after this adjustment, however, we observe ranges of the RGB band values to differ between the two imagery generations for the same location. For each location, we therefore create monthly target composites from images from the newer generation, to which we spectrally match images from both the older and newer generation. Specifically, we calculate 256 quantiles for each band in both individual old-generation images and the new-generation target composites and subsequently align distributions by scaling each quantile in the former to the value of the same quantile in the latter.

We then proceed to construct reference composites to serve as a comparison for each individual image. Our goal is a reference composite that for any given location and date resembles the appearance of that location when there is no market taking place. We therefore sample images that are temporally close – within ± 6 weeks of each image's acquisition date – and maximise contrast to potential market days by excluding images taken on the same day-of-week. From this initial sample, we select three copies of each of the two closest instances of every different day-of-week, two copies each of the next two closest instances and one copy each of the next two closest, giving us a maximum sample of

$$6 \text{ days of week} \times 2 \times (3 + 2 + 1) \frac{\text{images}}{\text{days of week}} = 72 \text{ images}$$

for each image's reference composite. Parts of each image in this stack may be masked out because of cloud cover. Therefore, the effective number of images available for aggregation in each pixel will be lower than 72. We then construct an 'interval mean'-composite from all pixels falling between the 40th and 60th percentile per band in the sample. In contrast to a canonical median composite, we found from inspection of the resulting difference images that this enlarged

window helps address low-level noise coming from remaining spatial misalignment between images.

This way of selecting imagery for the reference composites performs satisfactorily in areas where clouds and their shadows are seasonal or generally covering large areas. Visual inspection, however, revealed that despite the multiple pre-processing steps, composites were often still noisy in areas where clouds typically occur in small patches of cumulus clouds, such as along tropical coasts. Here, a larger share of pixels in the stack is masked and unmasked pixels are more likely to be affected by noise from shadows or remaining cloud fragments. To address this, we identify in each reference composite from the first iteration those pixels that have less than 36 valid pixels to aggregate over. For these, we expand the sample by the next six temporally closest images per day-of-week that are not already included in the first iteration. While this expansion reduces temporal proximity, climates with such cloud patterns tend to see little seasonality, suggesting that composites from more temporally distant images can still provide a good approximation of a non-market day's appearance.

By inspecting images across geographical contexts, we furthermore find that brightness variation alone – as represented by differences within each of the red, green or blue colour bands – does not capture well the colour variation associated with market activity relative to varying ground colours. We therefore calculate for each pixel a polar representation of its colour according to the following formulas:

$$\theta_1 = \arctan\left(\frac{\sqrt{red^2 + green^2}}{blue}\right); \quad \theta_2 = \arctan\left(\frac{green}{blue}\right)$$

θ_1 and θ_2 can be understood as angles between the individual bands identifying colours.

We then match each individual image to its reference composite and calculate the absolute difference within each of the three colour bands as well as their ratios θ_1 and θ_2 . As our goal is to identify areas with periodic changes, we then calculate another interval-mean composite between the 40th and 60th percentile of these difference images sorted by day-of-week and converted to

absolute values. In this representation, a pixel with a large value is one whose band value (red, green, blue, θ_1 , θ_2) is frequently different on a given day-of-week compared to other days.

We want to allow for both brightness and colour variation to indicate busier markets, and therefore multiply the maximum absolute difference across the RGB bands with the maximum absolute difference across the θ_1 , θ_2 bands. In this representation, a high value indicates a pixel where brightness and colour frequently differ from the reference composite.

Equipped with this representation of periodic differences across the extent of the candidate location – one difference image for each day of the week –, we then aim to extract areas with relatively high differences on any given day. We found that brightly reflecting surfaces, especially rooftops, regularly create artefacts in the difference images as their colour can change drastically when illuminated from different angles. These artefacts are sufficiently large and frequent to not be entirely addressed by our other averaging steps. To reduce their influence, we perform two additional cleaning steps: first, we smooth out local outliers within the difference image using a 5-by-5 pixel median kernel. Second, since noise from bright rooftops is presumably uniformly distributed across days of the week – while the market signal is not – we subtract from each individual difference image an average of all other days of the week.

We then turn the cleaned pixel-level representations of periodic differences into contiguous areas. Noting that they lack a natural unit, we observe typical ranges of values across the derived difference representations and define, based on inspection, a range of geometrically increasing threshold values as

$$\left\{ \left(\frac{t}{20} \right)^4 \mid t = 9, 10, 11, \dots, 34 \right\}.$$

We then extract all contiguous areas above each threshold, discarding those smaller than 50m^2 as these typically represent noise. Furthermore, we aim to eliminate spatial outliers – shapes that are identified far away from the main detected area in each location. For this, we identify for each candidate location the day-of-week and shape that is associated with the highest threshold value (a ‘peak’ in the difference image) and select for the same day the largest shape encircling this

‘peak’. We discard all shapes that do not intersect with this encompassing shape. This filtering step assumes that the area with the strongest signal represents the core area of a potential market and essentially restricts other possible market areas to be in the vicinity of the core.

In the section on the validation of the market detection approach, we identified the threshold value at which we jointly maximise the share of actual markets that we detect and the share of markets among the detected shapes (Fig. 2A). In order to detect as many markets as possible, however, we manually examine detected shapes to screen for false positives as well as false negatives. We perform this examination on all shapes in descending order of signal strength until for a given level we no longer detect any false negatives.

Activity tracking

Equipped with outlines of market extents under various threshold values, we turn to constructing measures of market activity. We here use all available images, including those on non-market days and those we discarded because of heavy cloud cover across the whole image tile earlier. The activity tracking follows much of the same logic as the market detection. We again construct temporally-relevant reference composites from relatively clean images, now also including images that cover less than 20 percent of the overall candidate location, but at least 10 percent of the detected market area.

In the resulting difference images, we reduce noise from outlier pixels using a 3-by-3 pixel median kernel. For each image, we then derive the sum across pixels of the product of absolute brightness and colour differences within each of the previously detected shapes, as well as their intersections.

The intersections allow us to identify areas where the market typically expands or contracts. Specifically, we rank the rings by the threshold value that defines them – sorting from rings nearest to the core of the market to rings further away – and construct for each ring the median activity reading on market days, as well as the 75th percentile reading on non-market days. We then define as the market fringe the smallest ring where median market day readings still exceed the

75th percentile of non-market day readings. The outer boundary of this ring defines the limits of the market area for which we construct the activity measures. To avoid very thin rings, we restrict the collection to intersections where the smaller of the areas in the intersection is less than 70 percent the size of the larger area. These areas can be associated with threshold values lower than the accuracy-maximising one from Fig. 2A.

The above procedure returns two outputs: First, the shapes of the identified market areas for each threshold level and day-of-week, and, second, a table where rows identify summed deviations in a given image and the identified preferred market extent.

Details of validation exercises and respective data collections - Figure 2

Figure 2 uses three sets of market maps for validation, each of them varying not just by country, but also by how they were collected and their intended purpose. The Kenyan dataset represents the marketplaces sampled for a study of trading behaviour²⁰ and was generously shared by the authors. The authors reported having consulted with local government authorities for a market map but ultimately resorted to conducting their own, ground-based mapping.

The Malawian dataset originates from a policy report²¹ and does not provide further detail on the approach for listing and selecting marketplaces. However, we noted that most locations represented in the map fall into relatively large settlements, such as district capitals.

The Mozambican dataset represents original data collected by the authors²². As part of a larger study, enumerators were tasked to travel throughout a set of districts in the Nampula and Zambézia provinces along predefined routes. Market locations were identified from informant interviews as well as direct observation by enumerators during their travels. The sample used for the validation exercise includes only those marketplaces that enumerators found to be in operation during their surveys in 2021-23 and that had, according to local informants, a distinct market day. Enumerators were also tasked to photograph these locations on the ground, allowing the assessment of false negatives.

All validation maps come in the form of point coordinates either taken directly at the marketplace or in the surrounding village. To mimic a situation where market locations are not known ex-ante, we manually draw polygons around the entire settlement containing the marketplace as identified from the Google Maps basemap and subsequently apply the detection algorithm.

Across datasets, we repeatedly detect areas at high threshold levels on days where the dataset does not indicate a market day. In two cases each in Mozambique and Kenya, we detect areas only on a day other than the designated market day. In one case in Malawi, the validation data lists two market days (Mondays and Fridays), yet we detect areas only on Tuesdays and Saturdays. Since in all these cases the detected areas overlap directly with locations that appear similar to other listed marketplaces we detect in VHR imagery, we update the validation data to feature the detected days instead of the initially designated ones. Fig. S8 illustrates the detected areas for these instances.

Figure 4

Across analyses involving the activity data, we need to ensure that the readings – which have no naturally interpretable unit – are comparable over time and correctly weighted when aggregated spatially or temporally. Intuitively, we aim to scale the readings such that within each marketplace and day of operation, their value equals 0 on average on non-market days and 100 on average on market days over a reference period. The chosen reference period may differ by application: for comparisons across markets, for instance, care should be taken that each market's chosen reference period should represent a relatively 'normal' year, e.g. without major conflict.

A complication stems from the seasonal distribution not just of market activity, but also the number of readings. Images (and thus, activity observations) tend to be more plentiful in seasons with relatively little cloud cover for a given location, and scarcer during the rainy season. A simple average across all readings would therefore be biased towards the less cloudy seasons and would fail to be comparable across locations with potentially differing seasons. We therefore fit a penalised univariate smoothing spline with an empirically chosen smoothing parameter

separately for both market day and non-market day readings as well as by sensor generation. We then normalize using these interpolated values over a given reference period, subtracting the non-market day mean, then scaling the market day mean to be 100. Figs. 4A-C show examples of these data.

Figure 5

Fig. 5A shows the time series of the activity measure for three regions of Ethiopia between 2018 and 2024. When considering a time series spanning the shift in sensor configurations between 20201 and 2021, we found that despite our harmonisation procedure, activity readings differ between satellite generations. These differences appear idiosyncratic by region, likely reflecting how the different sensors capture the different colours across marketplaces.

We therefore aim to harmonize the two series - intuitively, we want the activity series from the two sensors to show the same patterns. At a market level, however, individual readings are too temporally sparse and noisy to perform a direct harmonization. Instead, we derive equal-population subdivisions within regions (Ethiopia's admin-1 level) of up to 2.5 million people and match the means and standard deviations of the two activity series within the subdivisions across the months where each series makes up at least 20% of the total available imagery (mostly between November 2020 and May 2021). Relative to a harmonization at the admin-1 level, this procedure has the advantage of allowing the mismatch between the two activity series to differ across space. We note that for applications using only values pre-2020 or post-2021, such harmonization will not be necessary.

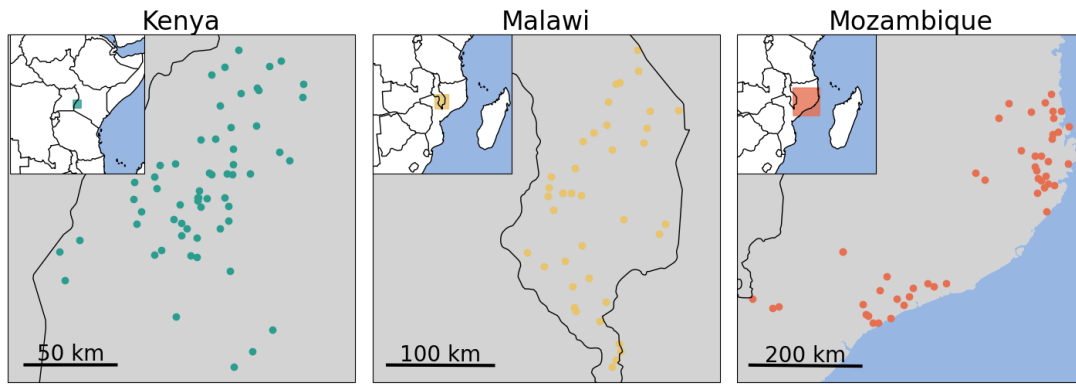


Fig. S1: Maps of validation datasets for market detection and activity tracking across three countries. Dots indicate locations of periodic marketplaces as recorded in reference datasets.

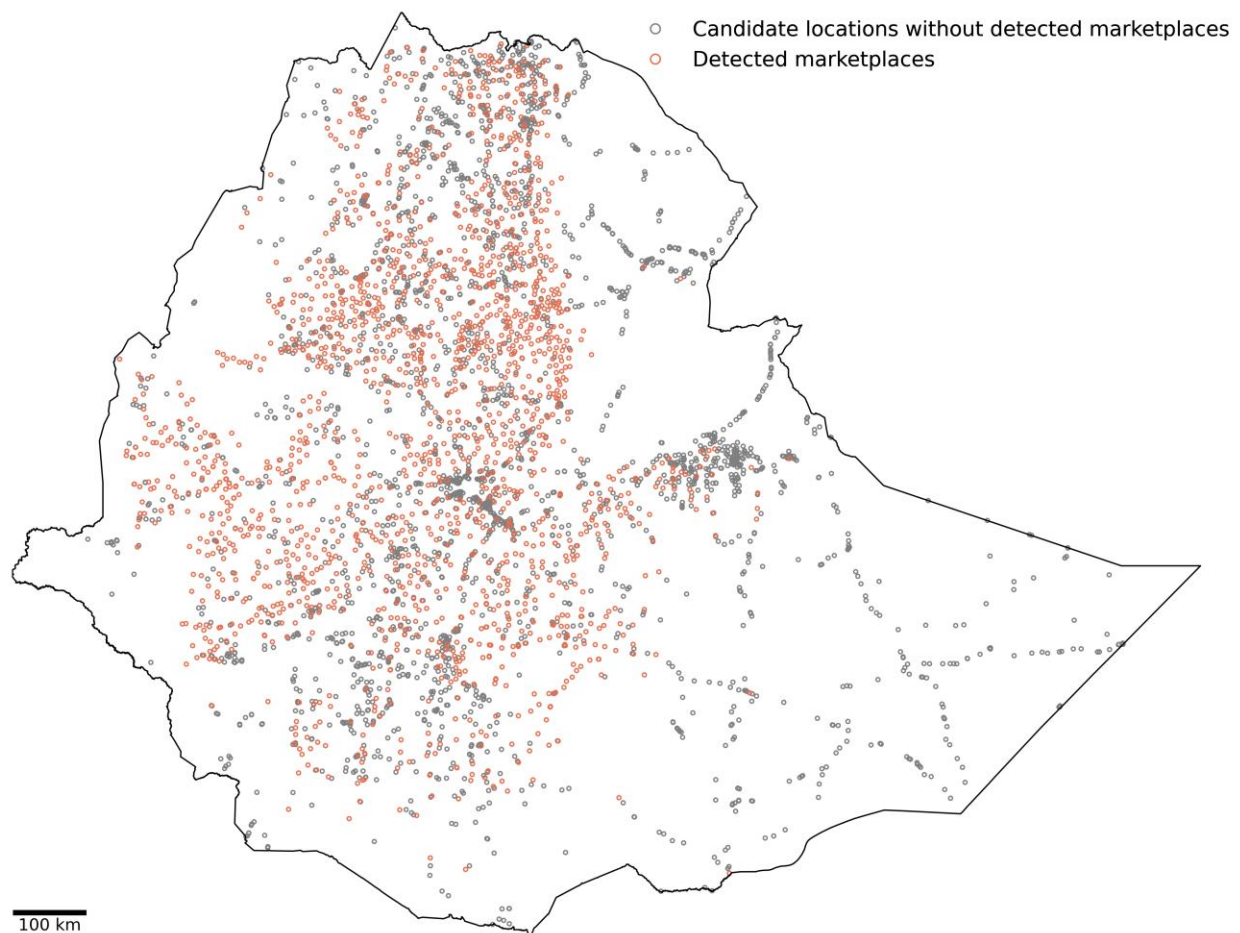


Fig. S2: Candidate locations and detected marketplaces in Ethiopia. Grey dots indicate locations where we applied our algorithm but did not detect periodic activity. We identified these ex-ante relatively likely market locations based on their periodic appearance changes in Sentinel-2 imagery. The orange dots indicate locations where we confirmed a marketplace.

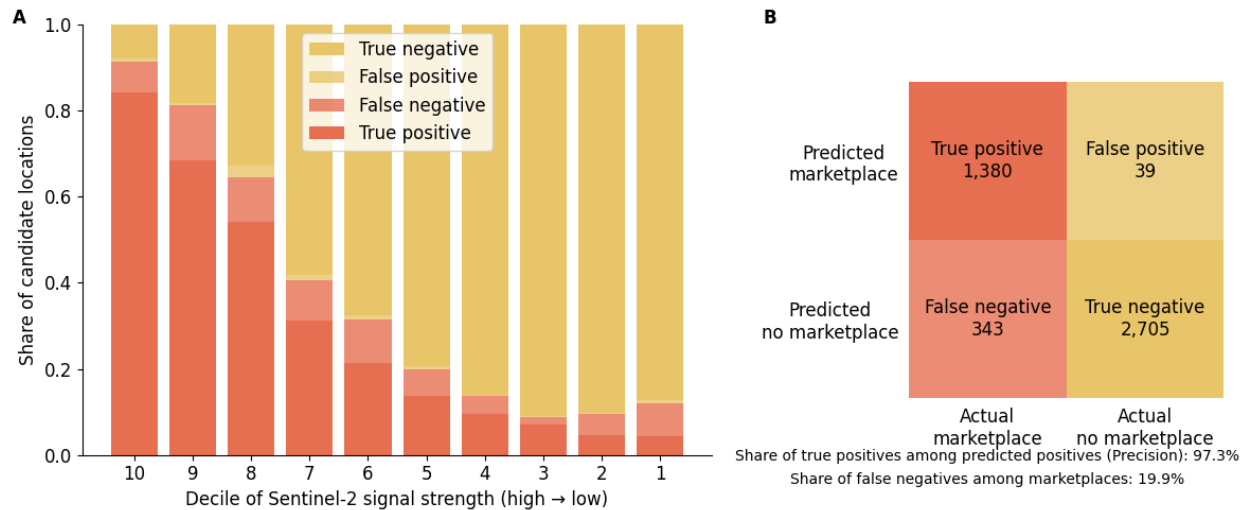


Fig. S3: Summary of screening procedure for marketplaces in Ethiopia. Panel (A) groups candidate locations into deciles according to their initial signal strength in Sentinel-2 imagery. Negatives and positives are classified according to the signal strength threshold from PlanetScope imagery shown in Fig (2). Subsequently, classifications are assessed as being true or false based on visual inspection of the detected shapes superimposed on VHR imagery. We note that the uptick in detection rates in the lowest decile is likely due to some marketplaces in the database originating from a manual search based on VHR imagery during the early stages of the research project. Panel (B) summarizes the exercise quantitatively.



Fig S4: Examples of detected market areas across four countries. (A) 14.35°N, 39.04°E; Ethiopia; Wednesday market (B) 11.6°N, 38.44°E; Ethiopia; Saturday (C) 0.23°N, 34.52°E; Kenya; Wednesday (green) and Saturday (red) (D) 1.62°S, 37.56°E; Kenya; Saturday (E) 16.2°S, 35.02°E; Malawi; Tuesday (green) and Saturday (red) (F) 15.02°S,

34.76°E; Malawi; Tuesday (G) 15.05°S, 40.31°E; Mozambique; Saturday (H) 13.96°S, 40.07°E; Mozambique; Saturday. Basemaps are from ESRI world imagery and show non-market days, except for panels (B) and (F), which are taken on the locations' respective market days.

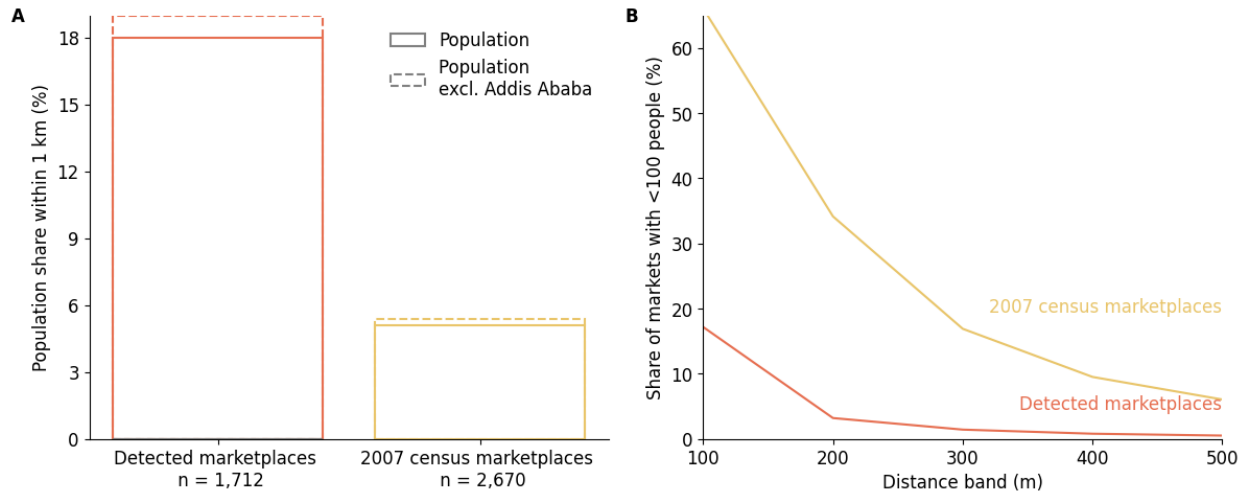


Fig. S5: Population counts surrounding marketplaces. (A) Repeating Fig. 3B with marketplaces from 2007 census. (B) Lines represent the share of marketplaces in the 2007 census and our dataset that have less than 100 people within some distance from their location, according to the GHSL layer²³.

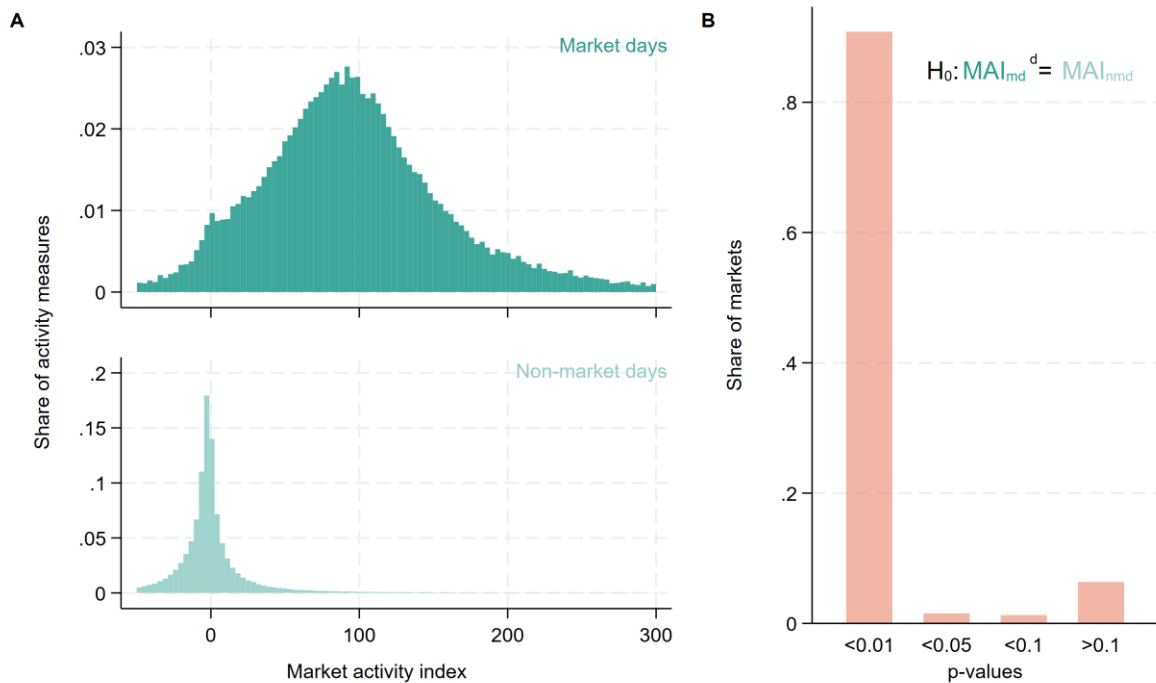


Fig. S6: Difference in distribution between market day measures and non-market day measures. (A) Histograms of market activity measures in 2018-2019 across detected marketplaces in Ethiopia. The measures are winsorized at (-50,300). (B) We perform two-sample Mann-Whitney tests for equality of distributions of the activity measures between

market days and non-market days within each marketplace. The height of the bars corresponds to the share of marketplaces for which the resulting p-value of the null hypothesis of equal distributions is below / above the respective values.

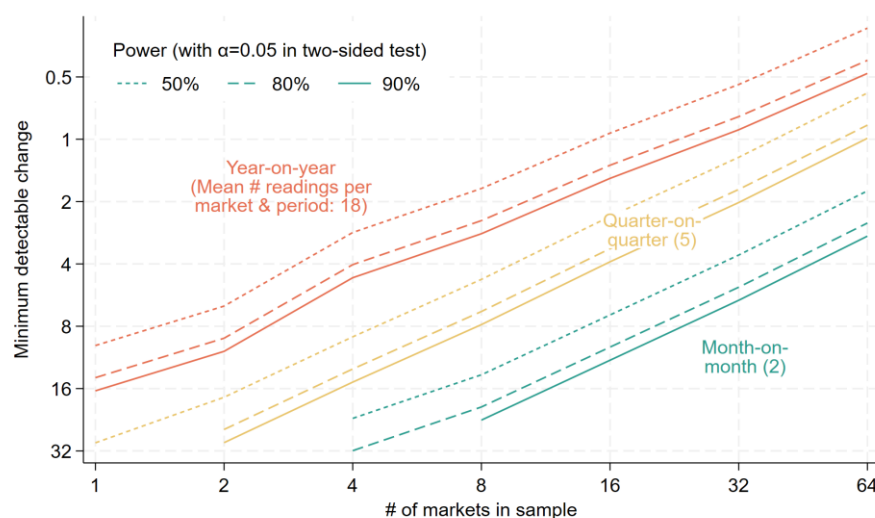


Fig S7: Power analysis to detect changes in market activity of various extents (vertical axis) with market samples of varying sizes (horizontal axis), depending on time period of aggregation (colours). Analysis is based on standard deviation of monthly means of market activity from randomly drawn market samples of the specified size in Amhara region for 2018-19.



Fig. S8: Validation markets with reassigned market days. For the shown locations, the validation data listed other market days than the sole ones on which we detect market activity, always in locations that appear highly similar to other marketplaces we detect. We therefore adjusted the validation data in these cases to reflect the high likelihood of falsely listed market days. **(A)** 1.03°N, 35.00°E; Kenya; Tuesday instead of Friday **(B)** 0.49°N, 34.84°E; Kenya; Monday instead of Friday **(C)** 15.13°S, 39.28°E; Malawi; Sunday instead of Tuesday **(D)** 16.97°S, 38.05°E; Malawi; Tuesday instead of Monday **(E)** 16.2°S, 35.02°E; Malawi; Tuesday and Saturday instead of Monday and Friday. Basemaps are from ESRI world imagery and show non-market days.

Supplementary Tables

Detected day:		<u>any</u>		<u>Fri, Sat or Sun</u>	
Number and share of detected areas within ... from religious building	50m	1	.06%	0	0%
	100m	5	0.3%	2	.3%
	250m	57	3.3%	23	2.9%
Total number of detected locations		1,712		795	
Distance to closest recorded religious building (km)	Mean			16.1	
	Median			12.1	

Tab. S1: Number and share of detected markets in vicinity of known religious buildings. We identify churches and mosques from OpenStreetMap's place-of-worship layer (29). The distance is calculated as the straight line between the detected market and the closest religious centre in the area. Friday, Saturday and Sunday are chosen as days when religious services may be held. We cannot reliably identify the denomination of each religious building and their associated days of worship.

Data & code availability

We access the satellite imagery used in the paper under an academic research user agreement from the provider, which prevents us from making the imagery available directly. We will, however, publicly deposit all code that extracts information from the imagery as well as the derived datasets and the code producing the figures in a GitHub repository.